Modeling and restoration of the coherent astronomical images distorted in atmosphere.

Yulia V.Zhulina

Interstate Joint Stock Corporation "Vympel", Moscow, Russia.

e-mail: yulia_julina@mtu-net.ru

Abstract.

The speckle-structures at output of the telescope optical system are modeled in this article. It is assumed that the telescope observes a satellite illuminated by a coherent light. The speckle-structures are obtained for several different sizes of the telescope aperture. The true image restoration is done by averaging the speckle-structures in the absence of the atmospheric distortions. Also, modeling of the speckle-structures in presence of atmospheric distortions is done. In this case, the true mage is restored by the algorithm using the multi-frame blind deconvolution. The algorithm does not use the preliminary restoring of the image spectrum and works without adaptive optics. But it can be used after the work of the adaptive optics. It is possible to restore the true image with the speckle- structures distorted in the atmosphere, if the optical system has the sufficiently good resolution. The results show that advantage of the telescope with high resolution predominates before the fact of extensive atmospheric distortions in the large apertures.

Introduction.

Speckle imaging techniques have been evolving since the fundamental idea was presented almost forty years ago[1,2]. The article [3] compares speckle imaging reconstruction results for several speckle imaging approaches. They compare four methods: 1) Knox-Thompson, using a hidden phase-finder in the object spectrum phase reconstruction [4,5,6]; 2) Knox-Thompson, using a phasor-based phase reconstruction; 3) Bispectrum, using only two bispectrum planes and a phasor-based phase reconstruction[7]; 4) Bispectrum, using four

bispectrum planes and a phasor-based phase reconstruction. In the simulations, the authors of [3] assume that the only aberrations are introduced by atmospheric turbulence and use parameters accordingly to work [8]. Reconstruction of the object spectrum in [3] is close to the methods used in [9,10].

In the work[11], it was shown that "turbulence noise" in the pupilnoise could be reduced by partitioning the telescope aperture and combining the bispectrum of all the subapertures. This was demonstrated with using simulation results. The work [12] continues this approach. The experimental results are received with using data from the 1.6 m telescope at the Maui Space Surveillance Site on Haleakala. Thus most of the research about speckle patterns is focused on the object spectrum phase reconstruction and uses the data separating on the pupil of telescope and processing the spectrums of all the subapertures.

Another fundamental engineering approach to the same goal is using of the adaptive optics systems. The article [13] reports the results obtained from the first adaptive optics system that deploys multiple laser guide beacons. The system is mounted on the 6.5 m Multiple Mirror Telescope in Arizona, and is designed to explore advanced altitude conjugated techniques for wide-field image compensation. Authors describe plans to develop the technology further on the twin 8.4m Large Binocular Telescope and the future 25 m Giant Magellan Telescope. The ground-layer adaptive optics (GLAO), was suggested by Rigaut [14] as a way to improve wide field imaging for large telescopes. Wavefront measurements from guide stars located far from each other (2–10 arc minutes) can be averaged to estimate the turbulence close to the telescope aperture. When the wavefront aberration is corrected by a single deformable mirror, the result is a partially corrected field that is as much as two orders of magnitude larger than the field achieved by the extant AO systems. The ground-layer adaptive optics can also be implemented using single laser guide star systems at smaller telescopes. For example, the 4.2m William Herschel Telescope has deployed one such a system [15] and the 4.1m Southern Astrophysical Research telescope is implementing another now [16]. However, the laser light in all these

cases does not come from infinity as starlight effectively does, and as the telescope diameter is increased, the mismatch in optical paths becomes so severe that no useful recovery of stellar wavefronts can be made. Hence a single-beacon GLAO implementation will not be effective for larger apertures [17]. In this case the multiple beacons can in principle provide the solution. The instantaneous stellar wavefront would be computed by a tomographic algorithm applied to the wavefronts measured from all the beacons[18-20]. This method, implemented with sodium beacon lasers, is planned for the Giant Magellan Telescope (GMT)[21,22], and for the Thirty Meter Telescope [23], to recover the full resolution of their apertures. Other approaches [24] use the method of the simulated restoration with modeling of the adaptive optics . The Starfire Optical Range 3.5 meter telescope has been artificially undersampled there and the multiframe blind deconvolution was used for imagery.

Modeling the speckle-structures in the optical system of a telescope is proposed in our article.

It is assumed that telescope observes a satellite illuminated by the coherent light. The speckle-structures are calculated for the several different sizes of the telescope apertures. In the all calculations the satellite is the same (Section1). In Section2, the true image restoration in the absence of atmospheric distortions is received by averaging the speckle-structures. Results are also obtained for the different sizes of the apertures. Modeling of the speckle-structures in presence of atmospheric distortions is given in Section3. Then restoration of the object image is performed by method, which was developed in [25] and applied to the real incoherent images in [26] (Section 4) . This algorithm does not use a priori data or any preliminary image spectrum recovery. Image is restored by the iterative algorithm with using the multi-frame blind deconvolution . Multi-frame blind deconvolution [27,28] reduces some of the problems by using multiple images of the same object,but with different blurring operators. Method of iterative calculations is based on the work [29].

1.Modeling the speckle structures.

Images obtained by a telescope in the coherent illumination differ from the images obtained under the Sun illumination even in the absence of any kind atmospheric distortions. When object is illuminated by the coherent light its image is formed by the object surface roughness comparable to the wavelength of light. The surface of object reflects light with an amplitude and a phase that depend on the slope and shape of each little piece of the roughness. In fact, in the coherent light we observe the microstructure of the object surface. Most strongly it can be seen in the surface ruptures. These places of the surface give the most sharp contrasts in the image. The most bright contrast can be seen on the lines of the contours of the object. The randomness of the field coming from the object arises from the randomness of the surface microstructure. The optical system of a telescope reproduces this microstructure with accuracy, defined by parameters of observation and resolution of the system. The result of observation is not the usual object picture, but a spotty image, called a speckle structure. A comprehensive discussion of the statistical properties of speckle, as well as detailed coverage of its role in applications is given in the book [30]. The more earlier book about the new optical methods based on the speckle-structures was [31]. We will take a photo of the Hubble satellite from the Internet (Fig.1) as the true image of the object for the all following calculations. Now we will describe the optical system of a telescope which observes the object in Fig.1.

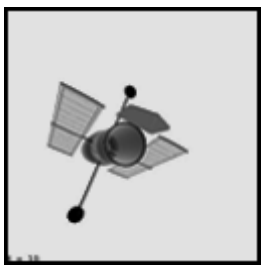

Fig.1 True image of satellite “Hubble”.

A general view of the object image at the output of telescope can be described by equation (A.14) (Appendix. A). Formula has a view :

$$I(\vec{\zeta}) = \left| \int_{-\infty}^{\infty} \tilde{K}_0(\vec{\zeta} - \vec{r}_{im}) t_0(\vec{r}_{im}) d^2 \vec{r}_{im} \right|^2 \qquad (1)$$

A variable $\vec{\zeta} = (\zeta_x, \zeta_y)$ is a vector of coordinates in the plane of the output image, a vector $\vec{r}_{im} = (r_x, r_y)$ is defined in (A.5) as the two-dimensional coordinate vector in the plane perpendicular to the telescope sight line, $t_0(\vec{r}_{im})$ is a complex field amplitude at the surface of the object and reflected by the object in direction of the sight line of telescope (A.4). $\tilde{K}_0(\zeta_x - r_x, \zeta_y - r_y)$ is the point spread function (PSF) of the optical system in the telescope (A.13). $I(\vec{\zeta})$ - is intensity of the image in the output image plane. In any optical system , with a coherent or incoherent illumination of the object , the same operations (1) are performed over the signal from the object. However, the results at output of the system with the coherent illumination are different from the results in the system with the incoherent illumination. The difference is that the output image (1) received in the incoherent object illumination is averaged by the random illumination. In a case of the coherent illumination it is only necessary to perform the exact calculations by formula (1).The following parameters were used at calculations: distance to the object $Range = 590km$ (this is the minimal distance to the satellite Hubble), diameter of the telescope aperture $D = 2.5m$ in Fig.2, $D = 3.5m$ in Fig.3, $D = 4.5m$ in Fig.4. $D = 5.5m$ in Fig.5, $D = 6.5m$ in Fig.6.

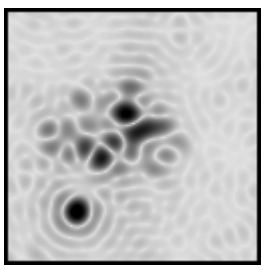

Fig.2 diameter 2.5m.

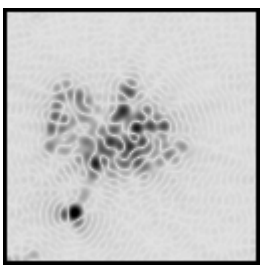

Fig.3diameter 3.5m.

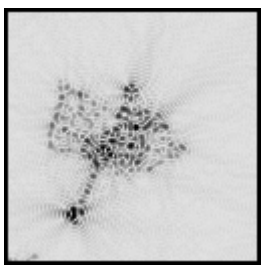

Fig.4 diameter 4.5m.

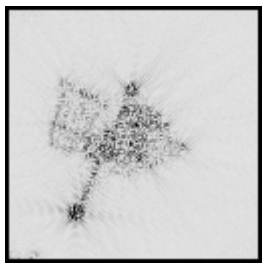

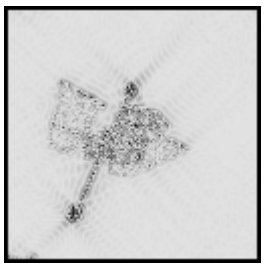

Fig.5 diameter 5.5 m. Fig.6 diameter 6.5m.

As the wavelength was taken value: $\lambda = 5.0 \cdot 10^{-7} m$. Resolution Δ_{res} in accordance with the formula $\Delta_{res} = \frac{\lambda \cdot Range}{D}$ is equal approximately to $\Delta_{res} = 12cm$ in the first case, and to $\Delta_{res} = 8.6cm$ - in the second, and $\Delta_{res} = 6.7cm$ - in the third. $\Delta_{res} = 5.4cm$ in the forth, $\Delta_{res} = 4.5cm$ - in the fifth . We have the same ranges in the all images (Fig.2-Fig.6). These are the speckle-structures , obtained in the coherent illumination. It is visible that beginning from the third frame (Fig.4) the speckle structure is similar to the actual image of the satellite, but there is not similarity in the first two images. It means that the speckle structure can give the image close to the true one if the telescope has a sufficiently high resolution.

2. Modeling averaging speckle structures.

It is known [30-31] that it is possible to receive almost the incoherent image by averaging the sufficiently large number of the speckle structures of the same real image. In this article it was tested as follows: K speckle structures were calculated for each diameter value. The wavelength was the same and equal to $\lambda = 5.0 \cdot 10^{-7} m$. The number of speckle structures $K = 100$. After receiving the all speckle structures there was made averaging over the all speckle structures in each case of the telescope diameter . As a result, we obtained the following images, shown in Fig.7-Fig.11 respectively, at $D = 2.5m$, $D = 3.5m$, $D = 4.5m$, $D = 5.5m$, $D = 6.5m$.

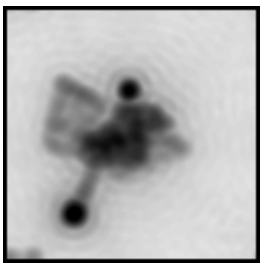

Fig.7 100 images, 2.5m.

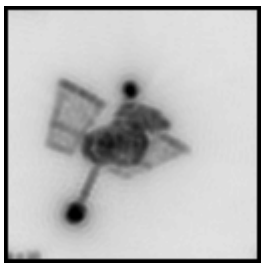

Fig.8 100 images ,3.5m.

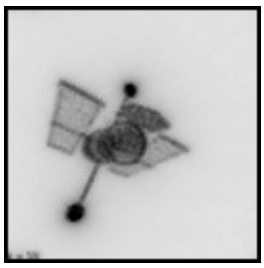

Fig.9 100 images, 4.5m.

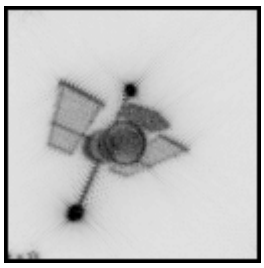

Fig.10 100 images, 5.5m.

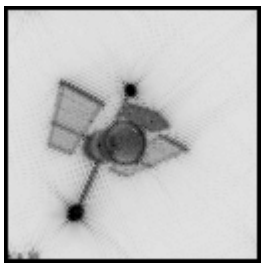

Fig.11 100 images ,6.5m.

From Fig.7-11 there is visible, that the images closed to the true one are received beginning from the telescope diameter $D = 4.5m$ (Fig.9). In Fig. 11 the full contour of the satellite image is received, it means that the image is restored in areas of the most contrasting parts of the object. Fig.7-11 show that the problem of speckle-structures can be resolved with sufficiently good resolution of the optical system and with diameter equal to $D = 4.5m$ (Fig.9) we begin to obtain the image close to the true one.

3. Modeling the atmospheric distortions.

The problem becomes much more complicated in the presence of the atmospheric phase distortions. The distorted speckle structures have been received in this case. For this purpose, the phase distortions were added to the telescope pupil $P(\vec{\rho})$ (Eq. A.8), and then the output image was calculated by formula (1). Below the Fig.12-16 show every the first of 100 distorted images obtained, respectively for the telescope diameters : $D = 2.5m$, $D = 3.5m$, $D = 4.5m$, $D = 5.5m$ $D = 6.5m$.

Modeling of phase distortions is described in Abstract B.

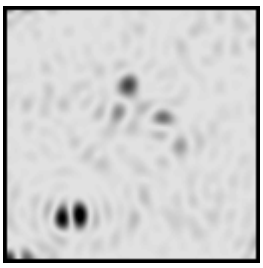

Fig.12 Distortions ,2.5m.

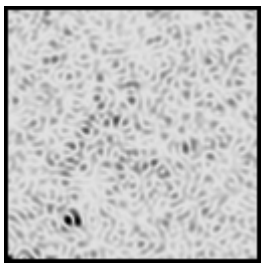

Fig.13 Distortions, 3.5m.

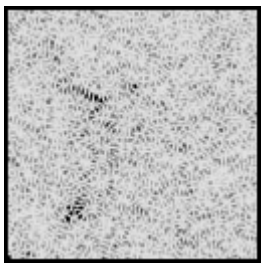

Fig.14 Distortions, 4.5m.

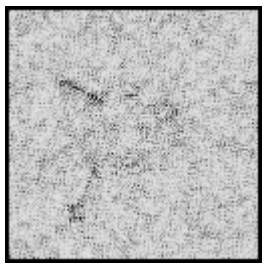

Fig.15 Distortions, 5.5 m.

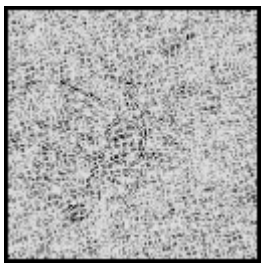

Fig.16 Distortions, 6.5m.

It is visible from the distorted images (Fig.12-16) ,that the contours of the object are lost and the loss is stronger when the telescope diameter is smaller .

4. Image restoration by the blind deconvolution.

There was made restoration of the distorted images. The algorithm of the multi-frame blind deconvolution derived in [25] was used. Below Fig.17-21 show the reconstructed images obtained respectively for the telescope diameters $D = 2.5m$, $D = 3.5m$, $D = 4.5m$, $D = 5.5m$, $D = 6.5m$ in each case with the 5 frames.

Fig.17 Restoration (2.5m).

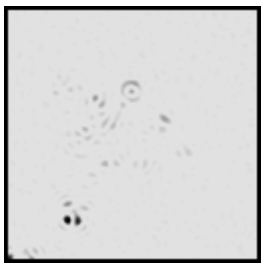

Fig.18 Restoration (3.5m).

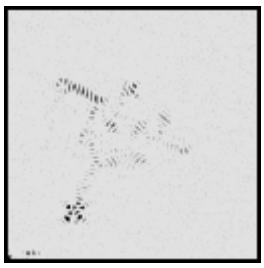

Fig.19 Restoration

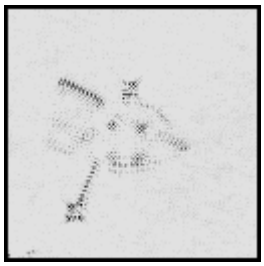

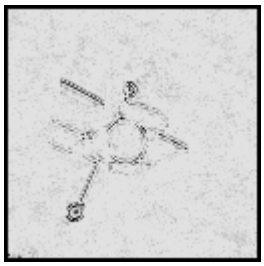

Fig.20 Restoration,5.5m, . Fig.21 Restoration,6.5m, .

Really it was the restoration by 100 distorted frames in each case of 5-th diameters . But every 20 frames were averaged before the restoration, so the deconvolution algorithm used only 5 frames obtained after averaging. The images are restored worse than images in the incoherent illumination[25-26]. We see that the contours of image has recovered better than other parts. The task of restoration in case of the speckle structures is twice as difficult, since the overlap of the two different distortions has place : the formation of speckles and the atmosphere distortions. But it is clear that restoration is better if the aperture of telescope is larger. In any case, the contours of the object can be recovered.

Conclusion.

The imaging by a telescope with observation through the atmosphere is modulated

in the article. The assumption is used that the a satellite is under the coherent light illumination. Averaging of the speckle structures in the absence of atmospheric distortions gives the satisfactory images close to the true satellite image.

Also the models for the speckle structures in the atmospheric distortions are received. The algorithm developed in [25] was used for the object image restoration in these conditions. As a result, we can conclude that the image restoration with the atmosphere distorted speckle structures is possible, but with the sufficiently good resolution in the optical system. The modeling shows that the satisfactory restoration of the basic object contours demands the aperture diameter larger than 4.5 meter if the range of the satellite is more than 600 km. The

advantage of the high telescope resolution predominates before the losses arising due to phase distortions in the atmosphere.

A plan to use large telescopes [13,15,16,21-23] seems quite reasonable. The works [11-12,14,17-20] are mainly focused on using of the adaptive optics. The proposed article does not require the preliminary restoring the true image spectrum, in other words, the algorithm works without adaptive optics. But the algorithm can be used also after receiving results of the adaptive optics.

Appendix A. Image on the output of the telescope optical system.

A signal reflected by the object can be written as follows. Denote the coordinate vector of a point on the object surface as $\vec{r} = (r_x r_y, r_z)$, the complex signal reflected from the surface at this point as $t_0(\vec{r})$ and position of the illumination source $\vec{r}_{source}$. In the incoherent systems of observation the illuminating source is the Sun, in the coherent systems the source is an artificial star or directly the ground-based laser. In these designations :

$$t_0(\vec{r}) = A_{reflect}(\vec{r}) \frac{\exp(jk|\vec{r} - \vec{r}_{source}|)}{|\vec{r} - \vec{r}_{source}|} E_{surf}(\vec{r}) \cdot \vec{n}(\vec{r}) \cdot (\vec{e}_0(\vec{r}) + \vec{e}_1(\vec{r})) \quad \text{(A.1)}$$

Here $A_{reflect}(\vec{r})$ is the random amplitude of the light coming from the object at point $\vec{r}$,

$k = \frac{2\pi}{\lambda}$ is the wave number, λ is wavelength of light, $E_{surf}(\vec{r})$ is the shape of the object surface. This shape can be represented by equation :

$$E_{surf}(\vec{r}) = \delta(r_z - f(r_x, r_y)), \quad \text{(A.2)}$$

where $\delta(x)$ is one-dimensional delta-function, $r_z = f(r_x, r_y))$ is the surface equation .

Further in (A.1): $\vec{n}(\vec{r})$ is the vector of the external normal to the surface of object at the point $\vec{r}$; $\vec{e}_0(\vec{r})$ and $\vec{e}_1(\vec{r})$ are the vectors of the point observation from the source of illumination $\vec{r}_{source}$ and the midpoint of the telescope aperture $\vec{\rho}_{lens}$ accordingly:

$$\vec{e}_0(\vec{r}) = \frac{\vec{r} - \vec{r}_{source}}{|\vec{r} - \vec{r}_{source}|}; \quad \vec{e}_1(\vec{r}) = \frac{\vec{r} - \vec{\rho}_{lens}}{|\vec{r} - \vec{\rho}_{lens}|} \quad ; \qquad \text{(A.3)}$$

$\vec{e}_0(\vec{r})$ and $\vec{e}_1(\vec{r})$ have modules equal to one.

(A.1) is a function of 3-dimensional argument $\vec{r}$. We will assume that coordinate r_z is the telescope sight line . The field reflected by the object in the direction of the telescope can be obtained by integrating (A.1) along the coordinate r_z . The result will be a signal $t_0(\vec{r}_{im})$ reflected by the object from the plane perpendicular to the line of sight:

$$t_0(\vec{r}_{im}) = A_{reflect}(\vec{r}_{im}) \cdot A_{im}(\vec{r}_{vis}) \qquad \text{(A.4)}$$

In (A.4) the two dimensional vector $\vec{r}_{im}$ is :

$$\vec{r}_{im} = (r_1, r_2) \qquad \text{(A.5).}$$

The 3-dimensional vector $\vec{r}_{vis}$ is : $\vec{r}_{vis} = (\vec{r}_{im}, f(\vec{r}_{im}))$;

The random amplitude $A_{reflect}(\vec{r}_{im})$ in (A.4) can be obtained at any point $\vec{r}_{im}$ with using the exponential distribution of the image intensity $P(I(\vec{r}_{im}))$ at this point.

The distribution is as follows:

$$P(I(\vec{r}_{im})) = \frac{1}{\bar{I}(\vec{r}_{im})} \cdot \exp(-\frac{I(\vec{r}_{im})}{\bar{I}(\vec{r}_{im})});$$

$I(\vec{r}_{im})$ is a random intensity of light reflected by the object at point $\vec{r}_{im}$;

$\tilde{I}(\vec{r}_{im})$ is an average intensity of light reflected by the object at this point. This average intensity can be taken as:

$$\tilde{I}(\vec{r}_{im}) = sqr(A_{real}(\vec{r}_{im}));$$

Under $A_{real}(\vec{r}_{im})$ we have in view an amplitude of the model image at point $\vec{r}_{im}$. This model image is used as true and is shown in Fig. 1.

As a result, the random amplitude $A_{reflect}(\vec{r}_{im})$ can be obtained from the exponential distribution in the form:

$$A_{reflect}(\vec{r}_{im}) = sqrt(I(\vec{r}_{im}))\ ,$$

and now it can be substituted into formula (A.4).

$A_{im}(\vec{r}_{vis})$ in (A.4) is equal to :

$$A_{im}(\vec{r}_{vis}) = \frac{\exp(jk|\vec{r}_{vis} - \vec{r}_{source}|)}{|\vec{r}_{vis} - \vec{r}_{source}|} \cdot \vec{n}(\vec{r}_{vis}) \cdot (\vec{e}_0(\vec{r}_{vis}) + \vec{e}_1(\vec{r}_{vis})) \quad \text{(A.6)}$$

The function $f(\vec{r}_{im})$ defined in (A.2) is an expression of the object surface. The function (A.4) represents the surface of the illuminated object. This signal (A.4) comes to the optical system , where the major operations are produced over it [32-33]: 1) the Fourier transform of the signal is obtained by the lens system (we assume a large distance of the object from the telescope, i.e. the Fraunhofer zone). 2)Detector of the receiver forms the intensity of the Fourier transform. 3) As a result, the output image of the telescope is obtained in the image plane .

Now we define the point spread function (PSF) of the telescope as $K(\vec{\zeta},\vec{r}_{im})$. Here $\vec{\zeta}=(\zeta_x,\zeta_y)$ is a two-dimensional vector in the image plane, the vector $\vec{r}_{im}$ was introduced in (A.5). In general case function $K(\vec{\xi},\vec{r}_{im})$ is given in [33]:

$$K(\vec{\zeta},\vec{r}_{im})=C\frac{\exp(j\frac{\pi}{\lambda z_0}|\vec{r}_{im}|^2)\exp(j\frac{\pi}{\lambda z_i}|\vec{\zeta}|^2)}{\lambda^2 z_0 z_i}\cdot \int_{-\infty}^{\infty}P(\vec{\rho})\exp(-j\frac{2\pi}{\lambda}(\frac{\vec{r}_{im}\cdot\vec{\rho}}{z_0}+\frac{\vec{\zeta}\cdot\vec{\rho}}{z_i}))d^2\vec{\rho} \qquad \text{(A.7)}$$

$\vec{\rho}=(\rho_x,\rho_y)$ is two-dimensional vector in the plane of the lens.

C - is constant,

z_i is a distance from the lens to the image plane,

z_0 is a distance from the lens to the object,

$P(\vec{\rho})$ is a function of the telescope pupil, which can be expressed in the simplest case by formula:

$$P(\vec{\rho})=\{\begin{matrix}0,if & \vec{\rho}\not\subset S_{\vec{\rho}}\\ 1,if & \vec{\rho}\subset S_{\vec{\rho}}\end{matrix} \qquad \text{(A.8)}$$

Here $S_{\vec{\rho}}$ is the surface of the lens aperture.

An image at the output of the telescope optical system in general case has a view [32-33]:

$$I(\vec{\zeta})=\left|\int_{-\infty}^{\infty}K(\vec{\zeta},\vec{r}_{im})t_0(\vec{r}_{im})d^2\vec{r}_{im}\right|^2 \qquad \text{(A.9)}$$

Here and everywhere below $d^2\vec{r}_{im} = dr_x dr_y$ (A.5) . Square of the modulus in (A.9) corresponds to the processing in the detector of optical system. $I(\vec{\zeta})$ is the intensity of the object image at the image plane. In formula (A.9) the square modulus of the phase multiplier $\exp(j\frac{\pi}{\lambda z_i}\left|\vec{\zeta}\right|^2)$ is present. So it can be neglected. There is also shown in [33] that the second phase multiplier $\exp(j\frac{\pi}{\lambda z_0}|\vec{r}_{im}|^2)$ can also be removed in the presence of the additional converging lens with appropriate focal length. Then we can write function $K_0(\vec{\zeta},\vec{r}_{im})$ instead of (A.7):

$$K_0(\vec{\zeta},\vec{r}_{im}) = \frac{C}{\lambda^2 z_0 z_i}\int_{-\infty}^{\infty} P(\vec{\rho})\exp(-j\frac{2\pi}{\lambda z_0}(\vec{r}_{im} + M\vec{\zeta})\cdot\vec{\rho})d^2\vec{\rho} \quad \text{(A.10)}$$

where

$$M = \frac{z_0}{z_i} \qquad \text{(A.11)}$$

is magnification of the optical system.

We introduce the new coordinates of the output image:

$$\vec{\xi} = -M\vec{\zeta} \qquad \text{(A.12)}$$

Then function $K_0(\vec{\zeta},\vec{r}_{im})$ becomes a difference of two arguments:

$$K_0(\vec{\zeta},\vec{r}_{im}) = \tilde{K}_0(\vec{\xi} - \vec{r}_{im}) = \frac{C}{\lambda^2 z_0 z_i}\int_{-\infty}^{\infty} P(\vec{\rho})\exp(j\frac{2\pi}{\lambda z_0}(\vec{\xi} - \vec{r}_{im})\cdot\vec{\rho})d^2\vec{\rho} \qquad \text{(A.13)}$$

As a result, we obtain instead of formula (A.9):

$$I(\vec{\zeta}) = \left| \int_{-\infty}^{\infty} \widetilde{K}_0(\vec{\zeta} - \vec{r}_{im}) t_0(\vec{r}_{im}) d^2 \vec{r}_{im} \right|^2 \quad \text{(A.14)},$$

where the variable $\vec{\zeta}$ is a vector of the point coordinates in the output image.

Appendix B. Modeling of phase distortions in images.

Atmospheric distortions are modeled by the standard method as follows below. There is considered a random phase process with the autocorrelation function having a circular symmetry [33]:

$$\gamma_\varphi(r) = \exp\{-(\frac{r}{W})^2\} \quad \text{(B.1)}$$

Here

$$r = [(\Delta x)^2 + (\Delta y)^2]^{1/2} \quad \text{(B.2)}$$

$$\Delta x = x_1 - x_2; \Delta y = y_1 - y_2;$$

Here the different phases have coordinates: $x_1, y_1; x_2, y_2;$

W in (B.1) is the width of the autocorrelation function of the phase.

From (B.1) we obtain the structural function $D_\varphi(r)$ in the form [3.3]:

$$D_\varphi(r) = 2\sigma_\varphi^2[1 - \gamma_\varphi(r)]. \quad \text{(B.3)}$$

Here σ_φ is a standard phase dispersion.

We assume that the random phase is modeled by a Gaussian random process with zero mean and variance equal to D_φ. Then, using formulas B.1 and B.3, we obtain in the first approximation:

$$D_\varphi(r) = 2\sigma_\varphi^2 \cdot (\frac{r}{W})^2 \quad \text{(B.4).}$$

Next, we assume that the image array has a size $N_0 \cdot N_0$, and each pixel is separated from the neighboring pixel by a distance equal resolution of the telescope $\Delta_{res} = \frac{\lambda \cdot Range}{D}$ (resolution is defined in the section 1). In this case, we assume that width W is the same in the direction x and the direction y and equal to:

$$W = \Delta_{res} \cdot N_0; \qquad (\text{B.5})$$

Now we assume that each pixel in the image has two-dimensional coordinates (x_k, y_l), where:

$$x_k = \Delta_{res} \cdot k; y_l = \Delta_{res} \cdot l; \quad \text{(B.6),}$$

Also, we assume the one-dimensional Gaussian distribution for the phase difference (B.2). Every pixel (x_1, y_1) will be defined with the number (k,l). Pixel (x_2, y_2), relative to which the value (B.2) is calculated , is selected as central point of the image with coordinates:

$$x_2 = \Delta_{res} \cdot N_0 / 2; y_2 = \Delta_{res} \cdot N_0 / 2; \quad \text{(B.7)}$$

Then the structural function $D_\varphi(r)$ can be expressed as $\tilde{D}_\varphi(k,l)$:

$$\tilde{D}_\varphi(k,l) = 2(\sigma_\varphi / N_0)^2 \cdot ((k - N_1)^2 + (l - N_1)^2) \quad \text{(B.8),}$$

where $N_1 = N_0 / 2;$

As a result , the random values $V_\varphi(k,l)$ can be obtained at each pixel

with the number (k,l):

$$V_{\varphi}(k,l) = Gauss(0, D_{\varphi}(k,l)); \qquad \text{(B.9)}$$

After this, the values $V_{\varphi}(k,l)$ are inserted into the space of the telescope pupil in the form of function $\exp(jV_{\varphi}(k,l))$. These functions give phases distorting the image.

References:

[1]A. Labeyrie, Attainment of diffraction limited resolution in large telescopes by Fourier analyzing speckle patterns in star images, Astron. Astrophys. 6, 85-87 (1970).

[2] D.Y.Gezari, A.Labeyrie and R.V. Stachnik, Speckle Interferometry: Diffraction-Limited Measurements of Nine Stars with the 200-inch Telescope.,Astrophys. J., vol. 173,April 1972, pp. L1-L5.

[3] Gregory C. Dente, Michael L. Tilton,Andrew P. Ongstad, Comparing Speckle Imaging Methods ,2009 AMOS CONFERENCE TECHNICAL PAPERS.

[4]K. T. Knox and B. J. Thompson, Recovery of images from atmospherically degraded short-exposure photographs, Astron. J. 193, p.45-48 (1974).

[5] K. T. Knox, J. Opt. Soc. Am., 66, 1236 (1976).

[6] G. C. Dente, Speckle Imaging and Hidden Phase, Appl. Opt, vol. 39, No. 10, pg. 1480-1485, 2000.

[7] G. R. Ayers, M. J. Northcott and J. C. Dainty, Knox-Thompson and triple-correlation imaging through atmospheric turbulence,J. Opt. Soc. Am. 5, 963-985 (1987).

[8] D. L. Fried, Optical resolution through a randomly inhomogeneous medium for very long and very short exposures, J. Opt. Soc. Am. 56, 1372-1379 (1966).

[9] R. H. Hudgin, Wavefront reconstruction for compensated imaging, J. Opt. Soc. Am., 67, 375-378 (1977).

[10] C. L. Matson, Weighted-least-squares phase reconstruction from the bispectrum, J. Opt. Soc. Am. A, 8, 1905-1913 (1991).

[11] B.Calef and E.Therkildsen , Improving large-telescope speckle imaging via aperture partitioning, 2008 AMOS CONFERENCE TECHNICAL PAPERS.

[12] Brandoch Calef, Speckle imaging with a partitioned aperture: experimental results, 2009 AMOS CONFERENCE TECHNICAL PAPERS.

[13] Michael Hart, N. Mark Milton, Keith Powell, Christoph Baranec,Thomas Stalcup, Eduardo Bendek, Don McCarthy, and Craig Kulesa, Wide-Field Image Compensation with Multiple Laser Guide Stars, Adaptive Coded Aperture Imaging, Non-Imaging, and Unconventional Imaging Sensor Systems, edited by Stanley Rogers, David P. Casasent, Jean J. Dolne, Thomas J. Karr, Victor L. Gamiz, Proc. of SPIE Vol. 7468, 74680L ,2009 .

[14] F.Rigaut, 2002, Ground-conjugate wide field adaptive optics for the ELTs, in Beyond Conventional Adaptive Optics, ed. E. Vernet, Proc. ESO 58, 11-16.

[15] O. Martin, 2008, Optomechanical commissioning of the GLAS Rayleigh laser guide star for the WHT, in Adaptive Optics Systems, eds. N. Hubin, C. Max & P. Wizinowich, Proc. SPIE 7015.

[16] A.Tokovinin, 2008, SAM – a facility GLAO instrument, in Adaptive Optics Systems, eds. N. Hubin, C. Max & P. Wizinowich, Proc. SPIE 7015.

[17] D.Andersen, 2006, Performance Modeling of a Wide-Field Ground-Layer Adaptive Optics System, PASP, 118, 1574-1590.

[18] R.Ragazzoni, E.Marchetti, F.Rigaut, Modal tomography for adaptive optics, A&A, 342, L53, 1999 .

[19] A.Tokovinin, M.Le Louarn, E.Viard, N.Hubin , R.Conan,
Optimized modal tomography in adaptive optics, A&A, 378, 710, 2001.

[20] M.Lloyd-Hart, N.Milton, Fundamental Limits on Isoplanatic Correction with Multiconjugate Adaptive Optics, JOSA A, 20, 1949,2003.

[21] N. Mark Milton, M. Lloyd-Hart, A. Cheng, J. A. Georges III, J. R. P. Angel, Design and expected performance of an MCAO system for the Giant Magellan Telescope, Proc. SPIE Astronomical Adaptive Optics Systems and Applications, ed. Robert K. Tyson and M. Lloyd-Hart, 5169, San Diego, CA, 2003.

[22] M. Lloyd-Hart, C. Baranec, N. M. Milton, T. Stalcup, M. Snyder, N. Putnam, and J. R. P. Angel, First tests of wavefront sensing with a constellation of laser guide beacons, The Astrophysical Journal, 634:679–686, 2005, November.

[23] R. G. Dekany, M. C. Britton, D. T. Gavel, B. L. Ellerbroek, G. Herriot, C. E. Max, J-P. Veran, Adaptive optics requirements definition for TMT, Advancements in Adaptive Optics, edited by D. B. Calia, B. L. Ellerbroek, and R. Ragazzoni, Proc. SPIE 5490, 879–890 (2004).

[24]. D. Gerwe, D. Lee, and J. Barchers, Supersampling Multiframe Blind Deconvolution Resolution Enhancement of Adaptive Optics Compensated Imagery of LEO Satellites, Proc. SPIE 4091, 187-205 (2000).

[25] Y.V.Zhulina,Multiframe blind deconvolution of heavily blurred astronomical images, Applied Optics, v.45, №28, October, 2006.

[26] Y.V.Zhulina, Extracting useful information from distorted images with multiframe blind deconvolution , 5 April 2007, SPIE Newsroom. DOI: 10.1117/2.1200702.0518

[27] Lane , Blind deconvolution of speckle images, J. Opt. Soc. Am. A, 9 , 1508-1514, 1992 .

[28] James G. Nagy, Veronica Mejia-Bustamante , MFBD and the Local Minimum Trap , 2009 AMOS CONFERENCE TECHNICAL PAPERS.

[29] G. R. Ayers and J. C. Dainty, Iterative blind deconvolution method and its applications, Opt. Lett., vol. 13, no. 7, pp. 547–549, July 1988.

[30] Joseph W. Goodman Speckle Phenomena in Optics: Theory and Applications, Roberts and Company, 2007.

[31] M.Francon ,Laser Speckle and Application in Optics, Academic Pr, New York, 1979,p.121.

[32] Joseph W.Goodman, Introduction to Fourier Optics, 3rd ed., Roberts and Company, Englewood, CO (2005).

[33] Joseph W. Goodman, Statistical Optics, John Wiley & Sons, (1985).